



A Capacitance Model for the Optically Controlled Short-Gate Length Non-Self-Aligned GaAs MESFETs with a Vertical Gaussian-Like Doping Profile

SHWETA TRIPATHI and S. JIT*

Centre for Research in Microelectronics (CRME), Department of Electronics Engineering,
Institute of Technology, Banaras Hindu University, Varanasi-221005, INDIA

*sjit.ece@itbhu.ac.in

Received 9 February 2011, Accepted 21 February 2011.

Abstract: - In the present paper, the internal capacitances of optically controlled short gate-length GaAs MESFETs with vertical Gaussian doped channel region has been modeled analytically. The photo effects on the short gate-length GaAs MESFET device capacitances have been modeled along with the electrical bias dependencies. The modeling has been done for linear as well as saturation region of device operation. The proposed model has been verified using ATLAS™, a 2D device simulator from SILVACO.

Key-Words: - Gate-source capacitance, Gate-drain capacitance Vertical Gaussian-Like doping profile, ATLAS.

I. Introduction

Optically controlled GaAs MESFET (GaAs OPFET) is the considered key device used for the design of photonic MMIC [1-3]. It is experimentally established fact that optical radiation incident on the transparent or semitransparent gate of the device is used to control the microwave characteristics of the OPFET [4-5]. It has also been investigated that many of the microwave characteristics of GaAs MESFET like resonant frequency, transit time etc., can be controlled by controlling the internal gate-source and gate-drain capacitances of the device [6-7]. Here it is worth mention that the level of incident illumination can change

the charge distribution under the gate that determines the internal capacitances of the

GaAs MESFET. Therefore the internal capacitances of GaAs MESFET can also be controlled by the incident illumination.

In the conventional microwave amplifiers and oscillators using GaAs MESFETs once the circuit is designed for a certain gain or resonant frequency, it cannot be changed except the value of some of the external component of the circuit is changed. But using optically biased GaAs MESFET provides us with means of one control terminal from which the microwave characteristics of the GaAs MESFET can be controlled by changing its internal capacitances.

A number of capacitance models for long channel optically controlled GaAs MESFET have been described [6, 8-10]. In view of the fact that for high speed and denser integrated circuits the device dimensions are getting smaller and with the reduction in device dimensions two dimensional (2D) effects become prominent. So in order to provide efficient simulations and accurate predictions of photonic microwave integrated system behavior having short gate-length MESFET devices, a careful development of an accurate model taking 2D effects into account is required. Some models for the capacitances of GaAs MESFET are present in the literature [7, 11-12] that considers two dimensional effects. Chhokra *et al.* [7] have reported an analytical model for the C-V characteristics of submicrometer GaAs MESFETs, considering 2D potential distribution contributed by depletion layer charges. Webster *et al.* [11] presented a new

empirical model whose structure is deduced from the reconstructed total charge function derived from the measured S-parameters of the device. Their model showed a good overall fit to the measured gate capacitance behavior of a commercial monolithic microwave/millimeter-wave integrated circuit (MMIC) MESFET over a wide range of bias conditions. It is interesting to note that the models reported so far for the short gate-length MESFET considered effect of electrical bias only and no optical bias dependency were included in any of the reported model. Keeping this fact in view, we reported a model [12] for internal capacitances of ion-implanted self-aligned short-channel GaAs MESFETs under dark and illuminated conditions. But that model ignores the effect of sidewall capacitances since the capacitances due to the sidewalls are negligible in self aligned GaAs MESFET device. Sidewall capacitances can play an important role while determining the internal capacitances of non-self aligned GaAs MESFET device. Therefore in the present work we have considered the sidewall capacitances while determining the overall internal capacitances of non-self aligned GaAs MESFET.

It is worth mention here that the modeling of Gaussian profile introduces the error function which is not fully analytical in nature. The error function is originated because of the non-integrable nature of the Gaussian function over some finite interval. Thus in the present work, an analytic Gaussian-like analytic function proposed by Dasgupta et al. [13] has been used in place of actual Gaussian profile to make the work fully analytical. The validity of the proposed model is shown by comparing the results with the numerical simulation data obtained by using the commercially available ATLAS™, a 2D device simulator from SILVACO [14].

II. Device Analysis

The device under consideration has been shown in Fig.(1) where a is the active channel thickness and L is the gate length.

Indium Tin Oxide (ITO) has been assumed as the gate metal because of its higher optical transmittance [15]. The monochromatic light ($\lambda \leq 0.87\mu\text{m}$) is incident on the Schottky gate-metal with photon flux density (Φ_o). The substrate of the device is assumed to be an undoped high pure LEC semi-insulating GaAs material. The active channel region of the device is an n-GaAs layer which is assumed to be obtained by ion implanting Si into the semi-insulating substrate.

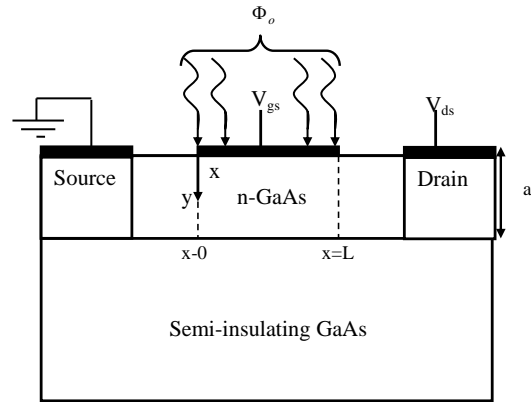


Fig. 1: Schematic structure of the GaAs MESFET where, L , a and Φ_o are the channel length, channel thickness and incident photon flux density respectively.

The ion distribution profile in the channel region can be given as [16]

$$N(y) = N_p \exp \left[- \left(\frac{y - R_p}{\sigma\sqrt{2}} \right)^2 \right] \quad (1)$$

where R_p is the projected range, σ is the projected straggle, and $N_p = \frac{Q}{\sigma\sqrt{2\pi}}$ is peak ion concentration in the substrate. Q is the dose.

The doping concentration in the channel can be given as [17]

$$N_d(y) = N_s + (N_p - N_s)F(y) \quad (2)$$

where N_s is the substrate doping concentration and

$$F(y) = \exp\left[-\left(\frac{y - R_p}{\sigma\sqrt{2}}\right)^2\right]$$

Since $F(Y)$ can not be integrated analytically, we have used an approximate analytic form of $F(Y)$ as [13]

$$F(y) \approx c_c \left[\left\{ a_c + \frac{2b_c\beta}{\sqrt{2}\sigma} (y - R_p) \right\}^2 - 2b_c \right] \times \exp\left[-\frac{a_c\beta}{\sqrt{2}\sigma} (y - R_p) - \frac{b_c}{2\sigma^2} (y - R_p)^2 \right] \quad (3)$$

where $a_c = 1.7857142, b_c = 0.6460835,$

$$c_c = 0.28\sqrt{\pi} \text{ and } \beta = \begin{cases} +1 & \text{for } y > R_p \\ -1 & \text{for } y < R_p \end{cases}.$$

When the light is incident on the gate metal carriers are generated within the semiconductor material. The generated electrons move towards the channel region and holes move towards the surface where they recombine with surface traps. Considering these effects of generation and recombination the net doping concentration can be given as [18]

$$N_D(y) = N_d(y) + G(y)\tau_n - \frac{R\tau_p}{a} \quad (4)$$

where $N_d(y)$ represents the doping profile defined by Eq.(2). R is the surface recombination rate, α is the absorption coefficient of GaAs material, τ_n and τ_p are the life time of electrons and holes, respectively and $G(y)$ is the photo-generation rate given by [16]

Under illumination, the optical radiation penetrates into the active layer of the MESFET which results in the generation of the excess electron-hole pairs in the active region of the MESFET. The excess holes generated due to illumination in the depletion region are swept out towards the metal side whereas the photo-generated

holes generated in the neutral region are diffused into the depletion region. These excess photo-generated holes in the neutral region as well as in the depletion region are finally swept out towards the metal at the Schottky gate. [10]. This gives rise to a photocurrent flowing from the semiconductor layer into the metal side that develops a photo voltage across the Schottky junction to make the junction forward biased. This photovoltage can be given as[19]

$$V_{op} = \frac{nkT}{q} \ln\left(1 + \frac{J_p(0)}{J_s}\right) \quad (5)$$

where J_s is reverse saturation current density at the gate depletion layer interface, n is the ideality factor of the Schottky junction, k is the Boltzman constant, T is room temperature(i.e., 300K), q is the charge of an electron, and $J_p(0)$ is the hole current density at the gate-channel interface[19]

III. Capacitance Modeling

We have assumed so far that the depletion region is confined only in the channel region below the Schottky gate and we have computed the 2D potential function accordingly. However, in practice, the depletion region below the gate has a very complicated structure and has extensions towards both the source and drain sides in a very complex manner depending on the bias conditions of the GaAs OPFETs [7,20]. We have considered the two simplified forms of the depletion regions corresponding to the linear and saturation regions of the GaAs OPFET shown in Fig.2a and Fig.2b respectively.

In Fig.2a, the region I represent the region with length L below the entire gate region where carrier velocity increases almost linearly with the increase in the applied drain source voltage V_{ds} . The regions IV and V in Fig.2a are the depletion region extensions towards the source and drain

[20]. Assuming the cylindrical shapes of the Regions IV and V as in Ref.[20] with radii L_1 and L_2 respectively, we write

$$L_1 = h(x)|_{x=0} \quad (6)$$

$$L_2 = h(x)|_{x=L} \quad (7)$$

where $h(x)$ is the depletion region height under the gate same as Ref.[12].

Since the depletion region extensions toward the source and drain shown in Fig.2(a) are assumed to be cylindrical in shape [19], and the heights of the depletion region in the Regions IV and V can respectively be described as

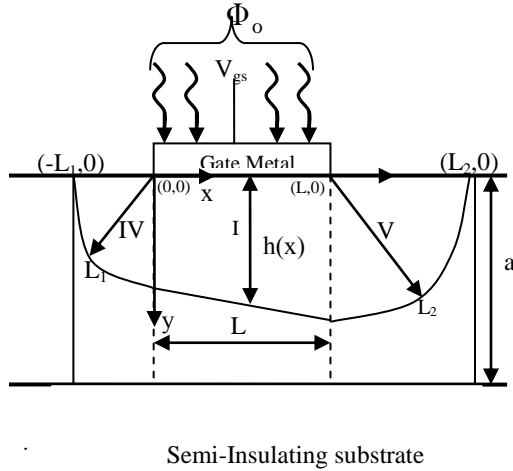


Fig. 2(a): Schematic diagram of the shape of depletion region of GaAs MESFET in linear region.

$$h(x) = \sqrt{L_1^2 - x^2} \quad \text{for } -L_1 < x < 0 \quad (8)$$

$$h(x) = \sqrt{L_2^2 - (x - L)^2} \quad \text{for } L < x < L + L_2 \quad (9)$$

In saturation region (see Fig.2b), the region I is the linear region similar to that of Fig.2a below the gate with length L_3 , Region II and III are the saturated parts of the channel (where the velocity of carriers are saturated)

with lengths L_s and L_{ex} and; region IV and V are the depletion region extensions toward the drain and source with the lengths L_4 and L_5 ; respectively. It may be noted that the onset of velocity saturation of the electrons has been assumed to be occurred at $x = L_3 < L$. Thus, the region $L_3 < x < L_3 + L_s$ (i.e. Region II) represents the portion of the saturation region confined below the gate and the region $L_3 + L_s < x < L_3 + (L_s + L_{ex}) = L_3 + L_{sat}$ (Region III) represents the extension of the velocity saturation region beyond the gate with $L_{sat} = L_s + L_{ex}$ representing the total length of the velocity saturation region in the channel [21]. The expressions for the L_s and L_{ex} can respectively be given by [21]

$$L_s = 2.06K_d \left(\frac{\epsilon_s (V_{ds} - V_{sat})}{q\sqrt{n_{cr}N_D(y)}} \right)^{1/2} \quad (10)$$

$$L_{ex} = 2.06(1 - K_d) \left(\frac{\epsilon_s (V_{ds} - V_{sat})}{q\sqrt{n_{cr}N_D(y)}} \right)^{1/2} \quad (11)$$

where K_d is a domain parameter, n_{cr} is the characteristic doping density of GaAs (typically $3 \times 10^{21} / m^3$) and V_{sat} is the minimum drain-source voltage required for the onset of velocity saturation given as[22].Following the same assumption of linear region the lengths of depletion region extensions towards source and drain in saturation region can be given as

$$L_4 = h(x)_{sat}|_{x=0} \quad (12)$$

$$L_5 = h(x)_{sat}|_{x=L} \quad (13)$$

where $h(x)_{sat}$ is the depletion region height under the gate in saturation region same as Ref.[20]. The depletion region heights in the IV and V regions (see Fig.2 (b)) are given as

$$h(x)_{sat} = \sqrt{L_4^2 - x^2} \quad \text{for } -L_4 < x < 0 \quad (14)$$

$$h(x)_{sat} = \sqrt{L_5^2 - (x - L)^2} \text{ for } L < x < L + L_5 \quad (15)$$

Now, the gate-source and gate-drain capacitances of the GaAs OPFETs can be defined as [7]

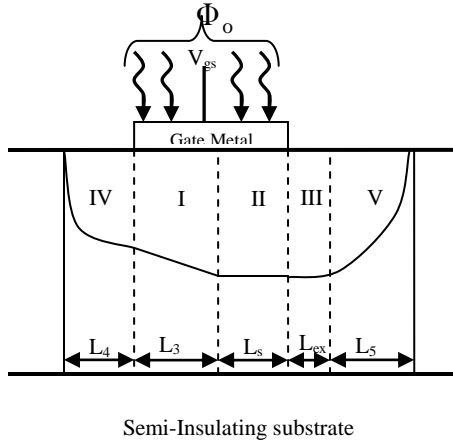


Fig. 2(b): Schematic diagram of the shape of depletion region of GaAs MESFET in saturation region.

$$C_{gs} = \left. \frac{\partial Q_t}{\partial V_s} \right|_{V_{gd} = \text{constant}} \quad (16)$$

$$C_{gd} = \left. \frac{\partial Q_t}{\partial V_{ds}} \right|_{V_{gs} = \text{constant}} \quad (17)$$

where Q_t is the total charge in the depletion under the gate of the device. Since depletion region charges are different for linear and saturation region due to the different structures of depletion region therefore in the following sections capacitance in linear as well as saturation region has been obtained separately.

3.1 Gate-Source and Gate-Drain Capacitances in Linear Region

The total charge Q_t in the depletion region under the linear region of operation of the device can be obtained by the addition

of the charges contained in region I, IV, V respectively. The charge in various regions of depletion can be evaluated using following relation [7]

$$Q = qZ \iint N_D(h(x)) dx dh(x) \quad (18)$$

Using above relation of charge in region I, IV and V, the total charge Q_t in the depletion region can be given as,

$$Q_t = Q_a + Q_b \quad (19)$$

where Q_a and Q_b are

$$Q_a = qZ \left[L_1 [K_1(h(0) - h(-L_1)) + M_1(h^2(0) - h^2(-L_1) + 2R_p(h(-L_1) - h(0)))] + L [K_1(h(L) - h(0)) + M_1(h^2(L) - h^2(0) + 2R_p(h(0) - h(L)))] \right] \quad (20)$$

$$Q_b = qZ L_2 [K_1(h(L + L_2) - h(L)) + M_1(h^2(L + L_2) - h^2(L) + 2R_p(h(L) - h(L + L_2)))] \quad (21)$$

where constants K_1, M_1 and N_1 can be given as

$$K_1 = a_c^2 c_c (N_p - N_s) - 2b_c c_c (N_p - N_s) + N_s - \frac{R\tau_p}{a} + \Phi_o \tau_n \exp(-\alpha R_p) \quad (22)$$

$$M_1 = 2a_c b_c c_c (N_p - N_s) (\sigma\sqrt{2})^{-2} \quad (23)$$

$$N_1 = \frac{\Phi_o \tau_n \exp(-\alpha R_p)}{\alpha \sigma \sqrt{2}} - a_c c_c (N_p - N_s) \quad (24)$$

Now, using Q_t (Eq.(19)) in Eq.(16) the expression for the gate-source capacitance C_{gs} in the linear region of operation can be given by

$$C_{gs} = P_1 L_1 + P_2 L + P_3 L_2 \quad (25)$$

where P_1 is the value of P with A' and B' calculated using $x_1 = 0, x_2 = -L_1$.
where P

$$P = qZ\sigma\sqrt{2} \left[\frac{A'}{\sigma\sqrt{2}} \left(K_1 - M_1 R_p (\sigma\sqrt{2})^2 \right) + M_1 B' \right] \quad (26)$$

Similarly, P_2 and P_3 are the values of P with A' and B' calculated using $x_1 = L, x_2 = 0$ and $x_1 = L + L_2, x_2 = L$, respectively. A' and B' are

$$A' = \left(\frac{qN_s}{\epsilon_s} \right)^{-1} \left[\frac{\sinh[k(L-x)]}{\sinh(k_1L)} + \frac{\sinh(k_1x)}{\sinh(k_1L)} - \frac{A''}{2A'''} \right]_{x_2}^{x_1} \quad (27)$$

A'', A''' are

$$A'' = \left[-\frac{2qN_s}{\epsilon_s k_1} \left(\frac{\sinh[k_1(L-x)]}{\sinh(k_1L)} + \frac{\sinh(k_1x)}{\sinh(k_1L)} \right) - 2 \times \right.$$

$$\left. (D_1 + D_2 - 2R_p) \left(\frac{\sinh[k_1(L-x)]}{\sinh(k_1L)} + \frac{\sinh(k_1x)}{\sinh(k_1L)} \right) \right.$$

$$\left. - \frac{4qN_s}{\epsilon_s} \right]_{x_2}^{x_1} \quad (28)$$

$$A''' = \left[\left((D_1 + D_2 - 2R_p)^2 - \frac{2qN_s}{\epsilon_s k_1} \times \right. \right.$$

$$\left. \left(\frac{\sinh[k_1(L-x)]}{\sinh(k_1L)} + \frac{\sinh(k_1x)}{\sinh(k_1L)} \right) V_{gs} - \right.$$

$$\left. \frac{2qN_s (\phi_{ch}(x) + D - (V_{bi} - V_{gs} - V_{op} + V_{ds}))}{\epsilon_s} \right]_{x_2}^{x_1} \quad (29)$$

$$B' = \frac{A'(D_1 + D_2 - 2R_p) - A'A'''}{2 \left(\frac{qN_s}{\epsilon_s} \right)^2} \quad (30)$$

Similarly, the gate-drain capacitance (C_{gd}) under the linear region of operation of the optically controlled GaAs MESFETs can be obtained using Q_t (Eq.(19)) in Eq.(17) as

$$C_{gd} = P_4 L_1 + P_5 L + P_6 L_2 \quad (31)$$

where P_4 is the value of P with $A^{I'}$ and $B^{I'}$ calculated using $x_1 = 0, x_2 = -L_1$. Similarly, P_5 and P_6 are the values of P with A' and B' calculated using $x_1 = L, x_2 = 0$ and $x_1 = L + L_2, x_2 = L$, respectively. $A^{I'}$ and $B^{I'}$ are

$$A^{I'} = \left(\frac{qN_s}{\epsilon_s} \right)^{-1} \left[-\frac{\sinh[k(L-x)]}{\sinh(k_1L)} - \frac{\sinh(k_1x)}{\sinh(k_1L)} - \frac{A^{I''}}{2A^{I'''}} \right]_{x_2}^{x_1} \quad (32)$$

$$A^{I''} = \left[\frac{2qN_s}{\epsilon_s k_n} \left(\frac{\sinh[k_1(L-x)]}{\sinh(k_1L)} + \frac{\sinh(k_1x)}{\sinh(k_1L)} \right) + 2 \times \right.$$

$$\left. (D_1 + D_2 - 2R_p) \left(\frac{\sinh[k_1(L-x)]}{\sinh(k_1L)} + \frac{\sinh(k_1x)}{\sinh(k_1L)} \right) \right.$$

$$\left. + \frac{4qN_s}{\epsilon_s} \right]_{x_2}^{x_1} \quad (33)$$

$$A^{I'''} = \left[\left((D_1 + D_2 - 2R_p)^2 + \frac{2qN_s}{\epsilon_s k_n} \times \right. \right.$$

$$\left. \left(\frac{\sinh[k_1(L-x)]}{\sinh(k_1L)} + \frac{\sinh(k_1x)}{\sinh(k_1L)} \right) V_{gs} + \frac{2qN_s}{\epsilon_s} \right.$$

$$\times \left(\phi_{ch}(x) + D - (V_{bi} - V_{gs} - V_{op} + V_{ds}) \right) \Big|_{x_2}^{x_1} \quad (34)$$

$$B^I = \frac{A^I (D_1 + D_2 - 2R_p) - A^I A^{I''}}{2 \left(\frac{qN_s}{\epsilon_s} \right)^2} \quad (35)$$

3.2 Gate-Source and Gate-Drain Capacitances in Saturation Region

In saturation region (see Fig.2b), the total charge in the depletion region can be obtained using similar methodology of linear region and can be given as

$$Q_t = Q_c + Q_d + Q_e \quad (36)$$

where Q_c , Q_d and Q_e are

$$Q_c = qZ \left[L_4 [K_1(h(0) - h(-L_4)) + M_1(h^2(0) - h^2(-L_4) + 2R_p(h(-L_4) - h(0)))] + L_3 [K_1(h(L_3) - h(0)) + M_1(h^2(L_3) - h^2(0) + 2R_p(h(0) - h(L_3)))] \right] \quad (37)$$

$$Q_d = qZL_s \left[K_1(h(L_3 + L_s) - h(L_3)) + M_1(h^2(L_3 + L_s) - h^2(L_3) + 2R_p(h(L_3) - h(L_3 + L_s))) \right] + qZL_{ex} \times \left[K_1(h(L_3 + L_s + L_{ex}) - h(L_3 + L_s)) + M_1(h^2(L_3 + L_s + L_{ex}) - h^2(L_3 + L_s) + 2R_p(h(L_3 + L_s) - h(L_3 + L_s + L_{ex}))) \right] \quad (38)$$

$$Q_e = qZL_5 \left[K_1(h(L_3 + L_s + L_{ex} + L_5) - h(L_3 + L_s + L_{ex})) + M_1(h^2(L_3 + L_s + L_{ex} + L_5) - h^2(L_3 + L_s + L_{ex}) + 2R_p \times (h(L_3 + L_s + L_{ex}) - h(L_3 + L_s + L_{ex} + L_5))) \right] \quad (39)$$

Now, the gate-source capacitance in saturation region of operation of the OPFET can be evaluated using Q_t (Eq.(36)) in Eq.(16) and can be given as

$$C_{gs-sat} = P_7 L_4 + P_8 L_3 + P_9 L_s + P_{10} L_{ex} + P_{11} L_5 \quad (40)$$

where P_7 is the value of P with A^I and B^I calculated using $x_1 = 0, x_2 = -L_1$. Similarly, P_8, P_9, P_{10} and P_{11} are the values of P with A^I and B^I calculated using $x_1 = 0, x_2 = -L_4, x_1 = L_3, x_2 = 0, x_1 = L_3 + L_s, x_2 = L_3, x_1 = L_3 + L_s + L_{ex}, x_2 = L_3 + L_s$ and $x_1 = L_3 + L_s + L_{ex} + L_5, x_2 = L_3 + L_s + L_{ex}$ respectively. A^I and B^I are same as given in Eq.(27)-Eq.(30) with $V_{ds} \rightarrow V_{sat}$.

Similarly, the gate-drain capacitance (C_{gd-sat}) under the saturation region of operation of the optically controlled GaAs MESFET can be modeled using Q_t (Eq.(36)) in Eq.(17) and can be written as

$$C_{gd-sat} = P_{12} L_4 + P_{13} L_3 + P_{14} L_s + P_{15} L_{ex} + P_{16} L_5 \quad (41)$$

where P_{12} is the value of P with A^I and B^I calculated using $x_1 = 0, x_2 = -L_1$. Similarly, P_{13}, P_{14}, P_{15} and P_{16} are the values of P with A^I and B^I calculated using $x_1 = 0, x_2 = -L_4, x_1 = L_3, x_2 = 0, x_1 = L_3 + L_s, x_2 = L_3, x_1 = L_3 + L_s + L_{ex}, x_2 = L_3 + L_s$ and $x_1 = L_3 + L_s + L_{ex} + L_5, x_2 = L_3 + L_s + L_{ex}$ respectively. A^I and B^I are same as given in Eq.(32)-Eq.(35) with $V_{ds} \rightarrow V_{sat}$.

IV. Results and discussion

To demonstrate the validity of the proposed model the theoretical results obtained for the internal gate-source and gate-drain capacitances of the GaAs OPFETs under dark and illuminated conditions have been compared with numerical simulation data obtained by ATLAS™ device simulator. For the numerical simulation data of dc capacitances, a 10mV ac signal with the frequency of 10Hz signal is applied at the

gate terminal of the device. The gate metallization has been assumed to be thin enough to allow 90% of the incident radiation to pass through. The incident optical power is 0.1 mW. The values of the other parameters used for computation of the model results are: $L = 0.25\mu\text{m}$, $a = 0.2\mu\text{m}$, $R_p = 0.1\mu\text{m}$, $V_{bi} = 1.01\text{V}$, $\sigma_p = 0.02\mu\text{m}$, $T_m = 0.9$, $\alpha = 10^6/\text{m}$, $\lambda = 870\text{nm}$, $N_p = 4 \times 10^{23}\text{m}^{-3}$ and $N_s = 1 \times 10^{21}\text{m}^{-3}$.

Variation of the internal gate-source capacitance (C_{gs}) and internal gate-drain capacitance (C_{gd}) with V_{gs} for linear region of operation under dark and illuminated condition is shown in Fig. 3 and Fig. 4. It is seen that both the capacitances increased with increasing incident illumination for a fixed gate-source voltage. This may be accounted by the fact that the depletion region width reduces under the illuminated condition.

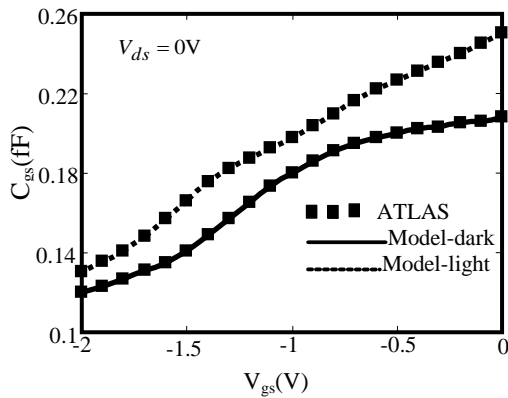


Fig.3: Plot of C_{gs} vs V_{gs} GaAs MESFET operated in linear region for dark and illuminated conditions

Figure 5 and 6 shows the gate-source capacitance (C_{gs-sat}) and gate drain capacitance (C_{gd-sat}) in the saturation region.

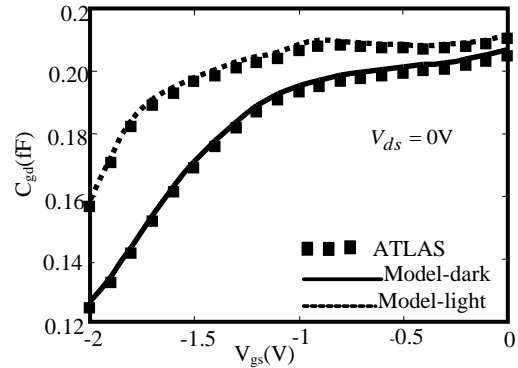


Fig.4: Plot of C_{gd} vs V_{gs} GaAs MESFET operated in linear region for dark and illuminated conditions

It has been found that C_{gs-sat} and C_{gd-sat} increases under illuminated condition. This may be due to the reduction in depletion width due to the photovoltage developed across the Schottky metal gate.

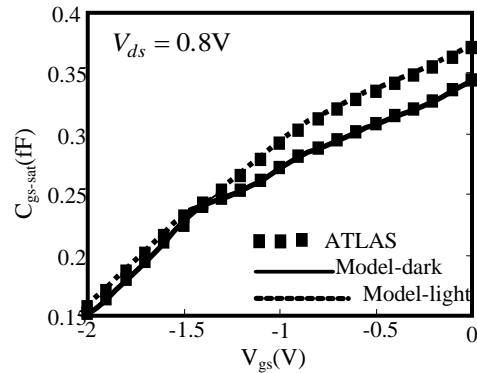


Fig. 5: Plot of C_{gs-sat} vs V_{gs} GaAs MESFET operated in saturation region for dark and illuminated conditions.

It can also be observed that C_{gs-sat} increases with the increase in V_{gs} because depletion region width decreases with the increase in gate bias (i.e. more positive V_{gs}). From Fig. (6) it can also be inferred that C_{gd-sat} decreases with the increase in V_{gs} like the conventional long channel device[23].

In Figure (7) gate-source capacitance has been plotted as a function of drain-source voltage (V_{ds}). It can be seen that gate-source capacitance becomes larger for illuminated condition. It can also be observed that gate-source capacitance decreases with the increase in (V_{ds}) in the linear region and becomes nearly constant in the saturation region.

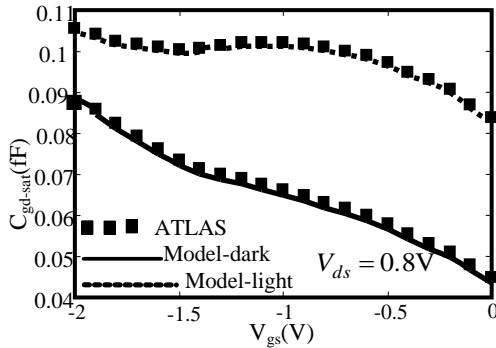


Fig.6: Plot of C_{gd-sat} vs V_{gs} GaAs MESFET operated in saturation region for dark and illuminated conditions.

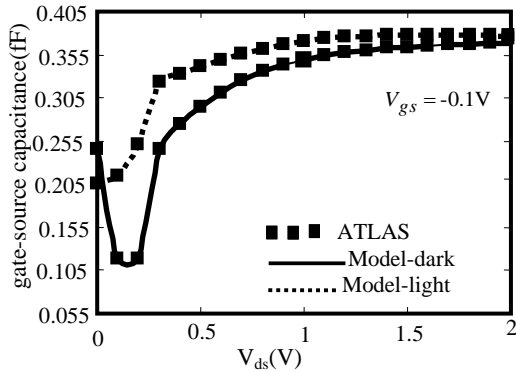


Fig. 7: Plot of gate-source capacitance vs V_{ds} of GaAs MESFET under dark and illuminated conditions.

Figure (8) shows the variation of gate – drain capacitance against the drain-source voltage (V_{ds}). Gate-drain capacitance increases with the increase in (V_{ds}) in the linear region and becomes nearly constant in the saturation region. Similar to the gate-source capacitance gate-drain capacitance is more under illuminated condition.

IV. Conclusion

A model for internal capacitances of GaAs OPFET has been developed. The charge for each part of the depletion region has been derived analytically for linear and saturation regions. The developed model may be suitably implemented for the design of photonic MMICs.

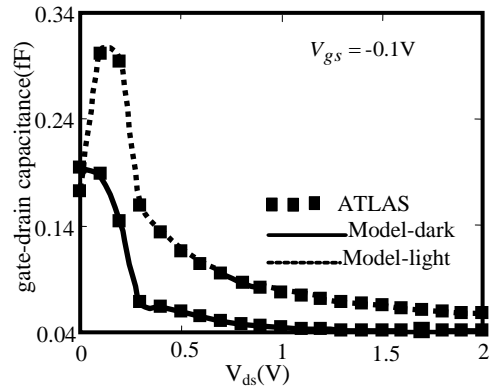


Fig.8: Plot of gate-drain capacitance vs V_{ds} of GaAs MESFET under dark and illuminated conditions.

References

- [1] J. Rodriguez-Tellez, K. A. Mezher, N. T. Ali, T. Fernandez, A. Mediavilla, A. Tazon, and C. Navarro, "Optically controlled 2.4GHz MMIC amplifier," Proceedings of the 10th IEEE International Conference on Electronics, Circuits and Systems, (ICECS) 2003., vol.3, 970, (2003).
- [2] J.M. Zamanillo, J. Portilla, C. Navarro and C. Pérez-Vega, "Optoelectronic control of a MMIC VCO at Ku band," in Proceedings of the 5th WSEAS International Conference on Electronics, Hardware, Wireless and Optical Communications, Spain, 138, (2006).
- [3] J. M. Zamanillo, J. Portilla, C. Navarro, and C. Perez-Vega, "Optical ports: next generation of MMIC control devices?," in proceedings of Microwave Conference, European, 1391, (2005).
- [4] A. J. Seeds and A. A. de Salles, "Optical control of microwave semiconductor devices," IEEE Trans. Microwave Theory Tech., 38, 577, (1990).

- [5] R. N. Simons, "Microwave performance of an optically controlled AlGaAsGaAs high electron mobility transistor and GaAs MESFET," IEEE Trans. Microwave Theory Tech., 35, 1444, (1987).
- [6] S. Jit and N. V.L. N. Murty, "Analytical study of the photo-effects on common-source and common-drain microwave oscillators using high pinch-off n-GaAs MESFETs" Microelectronics Journal, 37, 452, (2006).
- [7] S. A. Chhokra and R. S. Gupta, "Analytical model for C-V characteristics and transient response of submicrometer non-self-aligned GaAs MESFET," Solid-State Electronics, 42, 1917, (1998).
- [8] V. K. Singh and B. B. Pal, "Effect of optical radiation and surface recombination on the RF switching parameters of a GaAs MESFET," Optoelectronics, IEE Proceedings J, 137, 124, (1990).
- [9] C. Navarro, J. M. Zamanillo, A. M. Sanchez, A. T. Puente, J. L. Garcia, M. Lomer, and J. M. Lopez-Higuera, "An accurate photonic capacitance model for GaAs MESFETs," IEEE Transactions on Microwave Theory and Techniques, 50, pp. 1193, (2002).
- [10] N. V. L. N. Murty and S. Jit, "A new analytical model for photo-dependent capacitances of GaAs MESFET's with emphasis on the substrate related effects," Solid-State Electronics, 50, 1716, (2006).
- [11] D. Webster, M. Darvishzadeh, and D. Haigh, "Total charge capacitor model for short-channel MESFETs," Microwave and Guided Wave Letters, IEEE, 6, 351, (1996).
- [12] S. Tripathi and S. Jit, "A two-dimensional analytical model for the gate-source and gate-drain capacitances of ion-implanted short-channel GaAs MESFETs under dark and illuminated conditions" *J. Appl. Phys.*, in press.
- [13] A. Dasgupta and S.K.Lahiri, "A novel analytical threshold voltage model of MOSFETs with implanted channels," Int. J. Electronics, 61, 655, (1986).
- [14] ATLAS: Silvaco International 2008
- [15] S. A. Bashar, "Study of Indium Tin Oxide(ITO) for Novel Optoelectronic Devices," University of London, 1998.
- [16] S.M. Sze, Physics of semiconductor devices, second ed., Wiley, New York, 1981.
- [17] A. Dasgupta, S. K. Lahiri, "A two-dimensional analytical model of threshold voltages of short-channel MOSFETs with Gaussian-doped channels", IEEE Trans. Electron Deice, 35 , 390, (1988).
- [18] S. Bose, M. Gupta, R.S. Gupta, " $I_d - V_d$ characteristics of optically biased short channel GaAs MESFET", Microelectron J 32, 241, (2001).
- [19] S. Jit and B. B. Pal, "A new optoelectronic integrated device for light-amplifying optical switch (LAOS)," IEEE Transactions on Electron Devices, 48, 2732, (2001).
- [20] S.P. Chin, C. Y. Wu, "A new I-V model for short gate length MESFETs", IEEE Trans. Electron Dev. 40, 712, (1993).
- [21] Michael Shur, "GaAs devices and circuits", Plenum Press, New York, 1986.
- [22] V. L. N. M. Neti and S. Jit, "Analytical modeling of photo-effects on the S-parameters of GaAs MESFETs," Microwave and Optical Technology Letters, 48, 150, (2006).
- [23] T.H. Chen and M.S.Shur, "A Capacitance Model for GaAs MESFET's" IEEE Trans. Electron Deice, 32 , 883, (1985).